Chapter 6
Feedback design example: lightwave receivers

The previous chapters have discussed various theories and tools (measurement methods, algorithms) to analyze the response of circuits with feedback loops. They discussed the synthesis of compensation networks for stable feedback loops. When designing circuits, structured design methods are to be preferred, as in example the feedback network synthesis method proposed by Nordholt [406]. Parasitic effects deteriorate the overall performance, and they may even endanger the loop stability in the case of wideband feedback circuits.
When using *estimated* device models, it is utopian to believe that higher order wideband feedback loops designed from scratch will perform as expected from the initial analysis. In practice, *iterative* synthesis[1] must be used to improve the initial design. Various relevant parameters need to be extracted from the measured data (or *reliable* simulation) to gain insight into annoying parasitic effects. Study of these extracted values leads to modifications for improving the overall design. Where required, these steps must be repeated, converging eventually to optimal performance.

This chapter discusses the applications of our design tools using an example chosen from practice. It illustrates the suitability of our tools to the support of iterative synthesis of lightwave receivers, designed for more than 1 GHz in bandwidth .
An introductory section 6.1 reviews various receiver configurations and introduces current-current feedback. Section 6.2 is focused on maximal bandwidth performance to illustrate the use of the transfer tools introduced in chapter [2–5]. Section 6.2 focuses on low-noise performance and illustrates the application of our noise tools, introduced in chapter 7–9.

Highlights
Highlights of this chapter on lightwave receivers using current-current feedback, originated from this study, are:
- *Third order* feedback loops over more than 500 MHz bandwidth [608].
- *Second order* feedback loops over more than 1 GHz bandwidth, in combination, with *noise tuning*
- *Low-noise performance* while using low-cost discrete components (3 pA/√Hz average noise over 1 GHz bandwidth using 1.5 pF photo diodes).

These receivers are applied to various lightwave transmission experiments, including the international projects ESPRIT 2054 (UCOL), RACE 2024 (BAF [108]) and internal projects including COSNET [107].

[1] The words *iterative synthesis* are use to distinguish a design approach from *trial-and-error* methods. An iterative synthesis is the improvement of a design in a structured way rather than random changes of circuits.

6.1. Lightwave receiver configurations

Lightwave receivers use one or more photo sensitive transducers such as PIN diodes, avalanche photo detectors (APD), photo-multipliers and camera-tubes. Some of these may be preceded by an optical amplifier for improving overall sensitivity. This chapter is limited to photo-sensitive devices in which the output current (photo current) is proportional to the lightwave signal level of interest. Two photo sensitive devices in shunt, as used in balanced receivers, can be treated as a single device. To simplify matters, all our examples use single PIN diodes as the photo sensitive device, although the concepts are more widerly applicable. We will simply refer to all these devices as *photo-diode*. The pre-amplifier that amplifies the (electrical) signal current generated in the photo-diode is referred to as the receiver *front-end*.
For wideband lightwave receiver front-ends the basic design aspects are bandwidth, noise performance and large-signal behavior. Gain is of secondary importance since additional amplifiers may be used to increase the gain. The same applies for linearity considerations when digital signals are to be received.

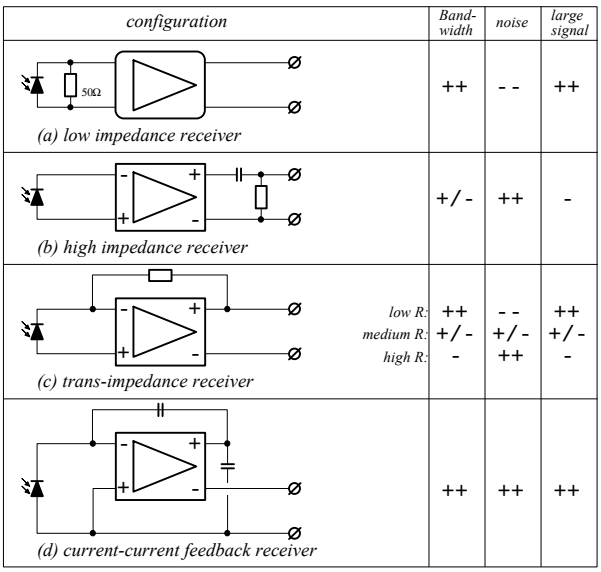


Fig 6.17 *A survey of various lightwave receiver front-ends*

Numerous lightwave receiver concepts have been published in recent years. A survey of various receiver front-ends is shown in figure 6.1. This classification facilitates the assessment of limitations on the basic design.

This section 6.1 discusses these four classes in more detail, to illustrate the choice of the configuration shown in figure 6.1d for the design example. Section 6.2 and 6.3 discuss various design aspects concerning wide-bandwidth and low-noise performance.

6.1.1. Conventional receiver front-ends

Low impedance receivers. The most simple lightwave receiver configuration is shown in figure 6.1a. The photo current is accurately transformed into a voltage using a resistor, prior to amplification.
This configuration is advantageous in that it enables the use of long transmission lines between photo-diode and amplifier. The detector load and the amplifier input impedance must be matched to the characteristic impedance of the cable, usually 50 Ω.
Another advantage is that any matched amplifier is applicable, since amplifiers with large bandwidth[2] and good large-signal performance are available.
The major disadvantage of low-impedance receivers is their poor noise performance. The thermal noise of the resistor usually exceeds the equivalent input noise of the amplifier, since it is as high as 18 pA/√Hz at room temperature when using 50 Ω resistors.

High impedance receivers. Removal of all low value shunt resistors and high value series resistors in the amplifier reduces the overall thermal noise contribution significantly. This includes all resistors biasing the photo-diode and the input amplifier stage. Figure 6.1b illustrates the configuration. This approach leads to relatively high amplifier input impedance, the photo-current to input voltage transfer being dominated by the photo-diode capacitance. The transfer function, which is integrating in nature, is usually equalized by adding a differentiating network to the amplifier output (see figure 6.1b).
The advantage of this concept is to be found in its ultimate low-noise performance. Bandwidth is mainly limited by the output network used to equalize the transfer function. The major disadvantage is that the receiver can easily be overloaded by low-frequency signals Of secondary importance is that harmonic distortion may exclude analog applications. This is because the transfer function is determined primarily by parasitic effects, and because the non-linear response of the transistor is not suppressed by feedback.

Transimpedance receivers. Some of the advantages of low- and high impedance receivers can be combined when using feedback [602]. The associated feedback configuration is shown in figure 6.1c. The transimpedance feedback loop controls the gain (and preferably also the bias) and transforms accurately the input current into an output voltage. The overall receiver performance is feedback dependent since the loop gain decreases with frequency in practical circuits. In figure 6.1c, three different feedback resistor values are considered: low, medium and high. They are:

- When the transimpedance resistance is chosen to be relatively low, its high thermal noise contribution will probably dominate the excess noise of the input stage. In this situation, the noise performance is poor as in the case of the low impedance amplifier. On the other hand, the feedback controls the gain over a wide bandwidth, since the loop gain is sufficiently high. As a result, this receiver has excellent bandwidth and large-signal performance.

[2] The corner frequency of the PIN-diode capacitance and the resistor may reduce the overall lightwave receiver bandwidth. For instance 1 pF shunted with 50 Ω resistance and another 50 Ω input impedance limits the bandwidth to 6.4 GHz

- When the transimpedance resistance is chosen to be relatively high, its low thermal noise contribution is comparable to that of the high impedance amplifier. The loop gain is relatively low so that the feedback is limited to low frequencies. The transfer function and the large-signal behavior are comparable to that of a high-impedance receiver.
- When varying the transimpedance resistance from low to high, the overall performance changes between the extreme values as described above. For medium transimpedance values all three basic aspects are realized with moderate performance.

Most lightwave receivers are currently configured as transimpedance receivers.

Principal restrictions of conventional receiver frontends. Telecommunication systems require frequency independent response and high dynamic range. Feedback is an adequate method to improve the response function as well as large-signal performance. Therefore, a transimpedance amplifier, with frequency independent transimpedance, is commonly used.
In the case of passive feedback networks, a frequency independent transimpedance network inevitably requires (noisy) resistors. When relatively high transimpedances are used, the thermal noise of the feedback network can be made small compared to the noise of the active devices. High transimpedance values, however, are associated with high overall gain and this gain restricts the overall receiver bandwidth. On the other hand, lowering transimpedance values improves the bandwidth at the cost of noise performance, due to increased thermal noise of the feedback network. Therefore, bandwidth, noise and large-signal performance cannot be optimized simultaneously for the conventional receivers in figure 6.1a,b,c.
These conventional receivers have in common that they transform input current into output voltage. Their gain is therefore not dimensionless, but has the dimension of an impedance. This dimension forms a principal limitation when optimizing bandwidth, noise and large-signal performance simultaneously.

6.1.2. Improved receivers with current-current feedback

This study has considered in depth alternatives to the above and has resulted in current-current feedback amplifiers. We introduced this feedback principle for wideband lightwave receiver design in [608]. Current-current feedback combines the bandwidth and large-signal performance of transimpedance amplifier, with the noise performance of high-impedance amplifiers. This principle replaces the noisy resistive feedback network of a transimpedance amplifier by a low-noise network such as a capacitive current divider. A specific implementation is shown in figure 6.1d.
The feedback loop, can be used to flatten the current-current gain frequency response and the amplifier can handle relatively large input signals, similarly to transimpedance amplifiers.

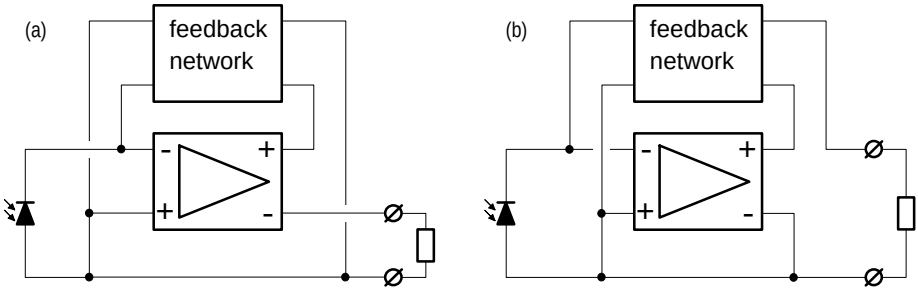
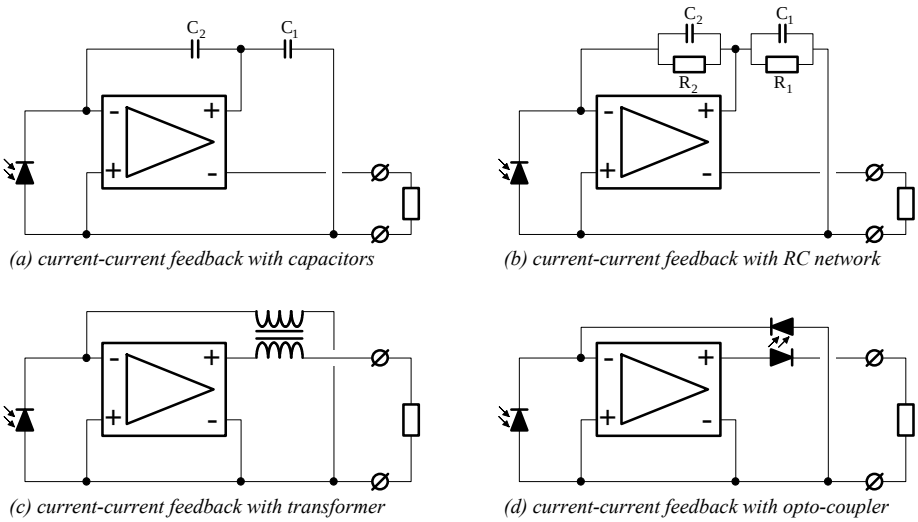


Fig 6.17 *Generic block diagrams of lightwave receivers using current-current feedback.*

Current-current feedback amplifiers require feedback networks, in shunt with the amplifier input and in series with the amplifier output. Figure 6.2 shows two block diagrams. The major difference is that in figure 6.2a the amplifier output port is floating to ground, while in figure 6.2b the feedback input port is floating.
The output signal is a current, which can be amplified with a second current-current stage or can be converted into a voltage using a load resistor.



(a) current-current feedback with capacitors

(b) current-current feedback with RC network

(c) current-current feedback with transformer

(d) current-current feedback with opto-coupler

Fig 6.17 *Specific implementation examples of lightwave receivers using current-current feedback*

Figure 6.3 shows various specific implementation examples of lightwave receivers using current-current feedback.

- The current gain α of the pure capacitive variant in figure 6.3a is controlled by the ratio of the two capacitors, or more precisely by $\alpha=(C_1+C_2)/(C_2)$.
- The RC-variant in figure 6.3b has some advantages to the configuration in figure 6.3a. It enables biasing of the input amplifier stage using the overall feedback loop. The resistors may be relatively high in value since the wideband feedback

performance is dominated by the two capacitors. Moreover, excessive voltages at low frequencies are avoided at the input node of the feedback network.
- The transformer variant in figure 6.3c eliminates the need for an amplifier with floating output terminals. The current gain equals the winding ratio of the transformer.
- The optical feedback variant, as is shown in figure 6.3d, circumvents the non-ideal performance of transformers while maintaining the advantage of non-floating amplifier terminals.

In the initial phase of this study, experiments were carried out using transformer current-current feedback. Bandwidths up to 100 MHz where shown to be feasible when transformers are used. Parasitic capacitances in the transformers limited the maximum bandwidth, and made further study uninteresting.
In the remainder of this text, design examples illustrating the implementation of current-current feedback amplifiers, using the RC-variant of figure 6.3b, will be considered.

6.1.3. Implementation of receivers using current-current feedback

The order of a feedback loop equals the dominant transfer order of the loop gain. The higher the feedback order is, the more complicated the design will be to control the stability of the loop. Therefore the loop order is in practice kept as low as possible.
In well-designed feedback amplifiers, each amplifier stage adds no more than one dominant pole to the loop while it provides maximum gain. In poorly designed feedback amplifiers, the gain per stage is significantly reduced in order to realize loops with low feedback order. This subsection discusses some well-designed feedback amplifiers having first-, second- and third-order feedback loops respectively.

First order loops. The simplest receivers with current-current feedback are similar to the first order configuration in figure 6.4a. A cascade of identical feedback amplifiers (figure 6.4b) increases the overall gain. Each loop consists of a single amplifier stage: two FET's in long-tailed pair configuration. This simple configuration has the advantage that stability compensation is not required.
On the other hand, the receiver performance is moderate because of the low loop-gain and because the amplifier stage must simultaneously match low-noise demands as well as output power requirements. We will pay no serious attention to these configurations.

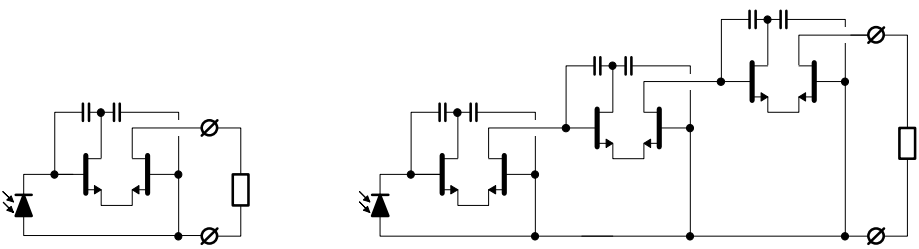


Fig 6.17 *AC diagram of a simple lightwave receiver using first order current-current feedback.*

Second order loops. Increasing loop gain by adding amplifier stages to the loop increases the available bandwidth and minimizes the noise contribution of the amplifier stages following the input stage. Figure 6.5 illustrates an implementation of overall current-current feedback over two amplifier stages. This study resulted in various receivers [608,108,607,609,610,612,613] using this configuration, with bandwidths in excess of 1 GHz.
A common-source configuration has been chosen for the first stage (T1), to maximize the loop-gain [406]. The design of T1 can be focused on optimal noise performance since the signal level to be delivered to the second stage is relatively low.
The second stage (T2+T3) is optimized for maximal output signal [406]. The current gain of this stage equals the current gain of transistor T2. Transistor T3 provides active decoupling[3] from the signal voltage at the collector of T3. This voltage is maximal at frequencies below $\omega<1/(R_1 \cdot C_1)$.
The output impedance of T3 is shunted to the input of the feedback network. Since T3 is configured in common base, its output impedance is relatively high and the deterioration of the feedback transfer by parasitic effects is relatively small. This property maximizes the overall loop-gain and makes T3 essential for taking full advantage of current-current feedback.
A phantom zero [406], as discussed in section 5.2, is used to controll the stability of the feedback loop,. This phantom zero is introduced by resistor R_{1s} that increases the feedback factor for frequencies above $\omega>1/(R_{1s} \cdot C_1)$.

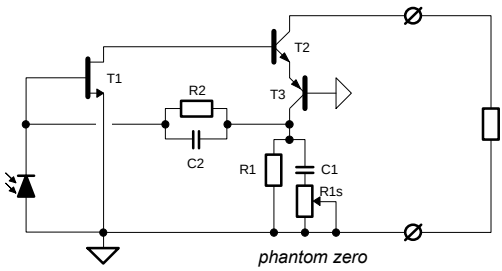


Fig 6.17 *AC diagram of a lightwave receiver using second order current-current feedback. Resistor* R_{1s} *introduces a phantom zero to improve the stability of the overall feedback loop.*

Third order loops. When a current gain greater than 100× is required in combination with bandwidths of several hundreds of MHz, two amplifier stages are unable to provide the required loop gain. Figure 6.6 shows a lightwave receiver reported using third order current-current feedback. The first lightwave receiver, using third order current-current feedback over several hundreds of MHz (500MHz, α=100×), was developed in the course of this study [608].

[3] Active decoupling is additional circuitry, like a buffer stage, for improving the isolation between output and input. Well-known examples are an inverting cascode stage (CE-stage, buffered by a CB-stage) and a non-inverting long-tailed pair (CC-stage buffered by a CB-stage). T2+T3 in figure 6.5 form a long-tailed pair. T4+T6 in figure 6.6 form a cascoded pair.

The input stage (T1) and output stage (T4+T5) are similar to the stages in figure 6.5. In this example, T6 has been added to the output stage to provide additional active decoupling of T4 from output signal variations at the collector of T6.
An intermediate stage (T2+T3) increases the loop gain. Transistor T2 provides the current gain, and transistor T3 provides the active decoupling of T2.
A phantom zero in combination with a pole-splitting network [406] are added to the loop to improve the overall loop stability. This compensation principle has been discussed in section 5.2.

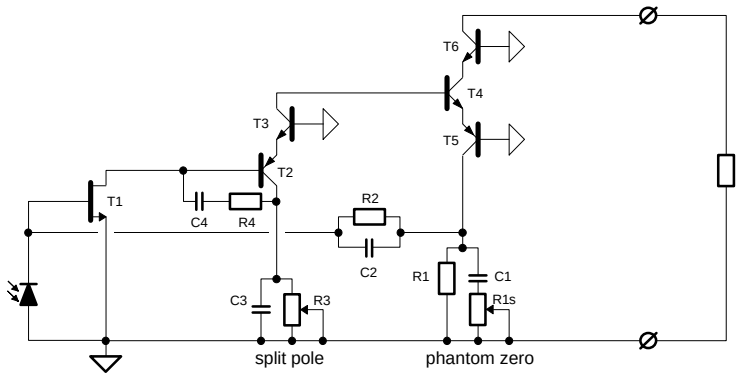


Fig 6.17 *AC diagram of a lightwave receiver using third order current-current feedback. Resistor* R_{1s} *introduces a phantom zero to improve the stability of the feedback loop. The local feedback network with* R_3, C_3, *and* R_4, C_4 *provides pole splitting for the same purpose.*

So far, various implementation examples are shown of lightwave receivers using current-current feedback. An exact description of their implementation is beyond the scope of this text. More relevant for this text is the *strategy* that has been used to handle circuit design of higher order feedback loops. Section 6.2 is focused on this strategy.

6.2. Iterative synthesis focused on maximal bandwidth

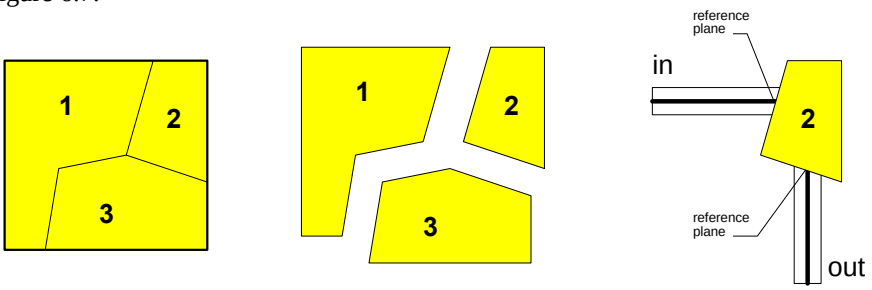
An important aspect of high-performance lightwave receivers is wide bandwidth. The use of overall feedback in amplifiers, covering several amplifying stages, is preferable to circuit configurations using local feedback in various individual amplifier stages [406]. In general, overall feedback increases the available bandwidth and improves the overall linearity of the amplifier [406].
One may conclude that the number of amplifier stages in the loop should, therefore, be chosen as high as possible. Unfortunately, the transfer order of the loop-gain increases with the number of stages, and higher order feedback loops set stringent demands on control of the loop stability. The number of stages in an overall feedback loop must therefore be limited in practice.
Higher order feedback loops are commonly avoided in wideband applications. In the literature, state-of-the-art receivers have been reported achieving more than 20 GHz bandwidth, using local feedback or no feedback at all. When bandwidth is the only design parameter to be maximized, this may be the best approach. When aspects such as

cost, noise, linearity and large-signal performance are relevant, then higher order feedback loops are to be preferred.

This section 6.2 focusses on a *convergent* iterative synthesis technique for designing *higher* order feedback loops (order ≥ 2) exceeding 1 GHz in bandwidth. Design examples, realized using discrete components mounted on glass-epoxy printed circuit boards (see section 1.4.1) illustrate the practicality of the method.

6.2.1. Quantifying parasitic effects using circuit stripping techniques

In the initial stage of the study of lightwave receivers (1985), synthesis methods proposed by Nordholt [406] were used for designing the basic circuit. Reasonable results have been achieved up to 100 MHz on lightwave receivers using second order current-current feedback loops. Empirical extension to greater bandwidths using a circuit simulator failed. This was traced to a too limited understanding of the circuit parasitics.
To facilitate a reliable simulation, a structured method has been developed for quantifying relevant parasitic effects. This subsection introduces a technique, termed *circuit stripping*, for locating inadequately modeled circuit elements and quantifying the associated error. It enables the extraction of improved models, as described in section 3.2, to adjust the overall circuit synthesis. The basic idea of circuit stripping is illustrated in figure 6.7.



(a) complete circuit, constructed constructed on a PCB (Printed Circuit Board).

(b) circuit is cut in individual pieces to facilitate two-port measurements well-defined reference planes

(c) piece '2' is measured as two-port between reference planes

Fig 6.17 *The basic idea of circuit stripping. The printed circuit board (PCB) has been cut into pieces to isolate individual sub-circuits. Each piece of PCB is extended with microstrips to facilitate full two-port measurements observed from well-defined reference planes.*

Consider a circuit for which the simulation fails above a certain frequency. Figure 6.7a represents this circuit, constructed on a printed circuit board (PCB). The printed circuit board (PCB) has been cut in several pieces, as is shown in figure 6.7b, to isolate individual sub-circuits. The sub-circuits of interest are then to be extended with microstrip lines with equal and precisely known length, as is illustrated in figure 6.7c. This construction facilitates an exact positioning of reference planes for full two-port measurements, as described in section 3.1.3 and 3.2.1.

A practical implementation of the approach is illustrated in figure 6.8. The center of this photograph shows a lightwave receiver, using third order current-current feedback (the configuration of figure 6.6). The printed circuit board (PCB) has been cut in four pieces: the three individual amplifier stages and the overall feedback network. In figure 6.8, they are arranged around the receiver.
Full two-port measurements on each piece of PCB facilitate the 'reconstruction' of the complete circuit in a simulator. When all pieces are measured, the reconstructed overall transfer is adequately predicted. On the other hand, step-by-step substitution of each piece of PCB by an equivalent circuit model provides the means for identifying poorly modeled circuit elements. These steps are then repeated on a reduced scale until all suspected circuit elements have been singled out. The measured data may then be used to improve the associated model of these elements.

Using this circuit stripping technique, it became clear that the validity of commonly used hybrid-Π models for bipolar transistors is quite limited. The focus of the study was shifted in turn, albeit temporarily, to transistor characterization, resulting in improved BJT models as discussed in section 3.2.2.
Circuit-stripping of our lightwave receiver design have been proven in practice to detailed, quantitative insight into various parasitic effects. Some of them to be reproducible quantities and are used to control the overall gain. Other identified parasitic effects have been reduced by careful redesign of the PCB layout.
An example is capacitance C_2 in figure 6.5 and 6.6. The parasitic stray capacitance over R_2 is a reproducible quantity for a given PCB layout and serves the purpose of feedback capacitance C_2.
Other examples are the parasitic effects originating from transistor T6 in figure 6.6. This transistor has been added to the circuit for providing adequate active decoupling of transistor T4 from signals at the collector output of T6. This is sometimes referred to as reducing the 'Miller' effect by a cascode configuration. Above a certain frequency, the benefits of T6 fade into insignificance and introduce new parasitics that are more harmful. As soon as this effect was identified and T6 was removed, the loop was compensable over a significantly wider frequency band.

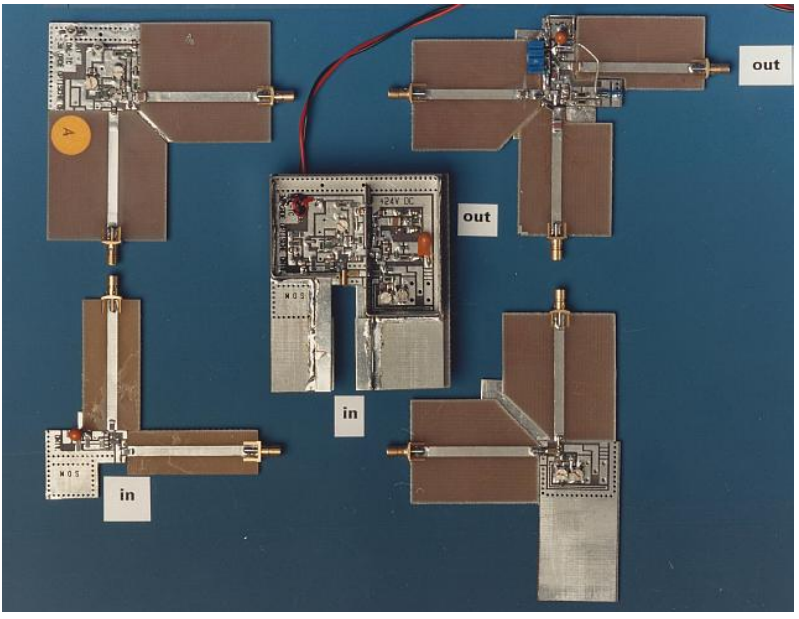


Fig 6.8 *Example of circuit stripping. The printed circuit board (PCB) of this receiver has been cut into pieces to isolate the three amplifier stages and its overall feedback network. Each piece of PCB is extended with microstrips to facilitate transfer measurements observed from well-defined reference planes.*

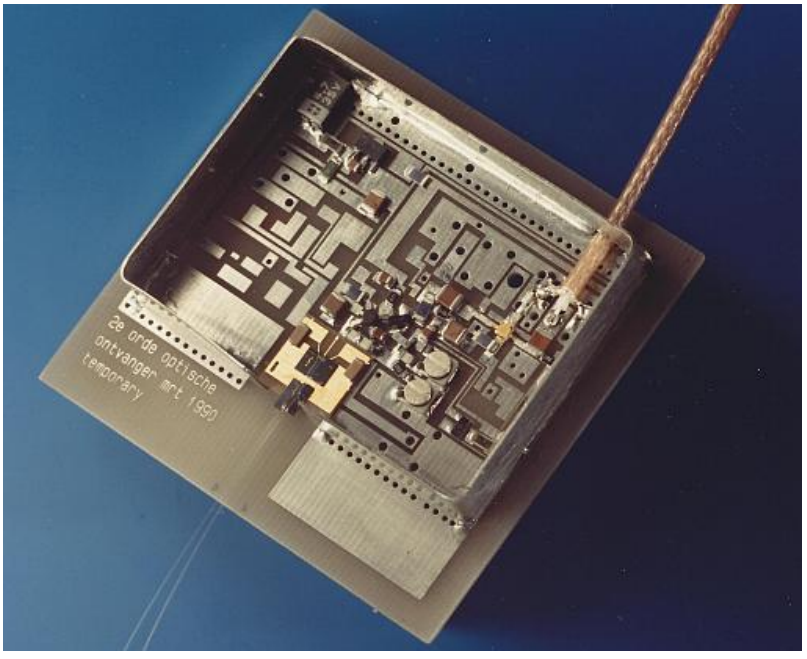


Fig 6.9 *Lightwave receiver (balanced) using second order current-current feedback. All components being no part of the receiver pre-amplifier have been omitted.*

6.2.2. Cumulative quantification of parasitics using pole-zero techniques

The *quantification* of individual parasitic effects, is merely one aspect of iterative synthesis. This facilitates reliable circuit simulation without distinguishing harmless parasitics from dominant parasitics. *Cumulative* quantification of the combined effect of various parasitics is required in order to whether particular parasitics are significant or not when combined. This cumulative assessment is essential because parasitic effects that are significant in specific sub-circuits or devices are not necessary of importance in the overall feedback loop.

In an integrated design environment, facilitated allowing acquisition and computer analysis of measured two-port parameters, designers are to quantify and cumulate parasitics with ease and in a structured way. Pole-zero extraction techniques, are eminently suitable for cumulative quantification parasitics from properly measured or simulated data. An experimental design environment, termed SABEL-CAE [111] and discussed in section 1.4.2, has been realized with many of the desired features.
In the future circuit simulators may support pole-zero techniques similar to that described herin. The designer simulates the circuit in two parts: a four-port feedback network and a two-port forward amplifier. The simulator evaluates the superposition model of the feedback circuit, as described in section 4.2, and extracts the dominant poles and zeros of the feedback loop. This is the desired cumulative quantification of parasitic effects.
When requested, the simulator provides the transfer function(s) of the compensation network(s), as described in chapter 5.

For an in-depth discussion of the associated algorithms see chapter 4 and 5. More effort has been spent on developing algorithms and software tools for pole-zero analysis and parameter extraction from measured data than was spent on the actual design of our lightwave receivers. Therefore, a short overview is given below to indicate the scale of this effort.

- From the very beginning the importance of measurements for improving the overall circuit simulation was evident. Therefore, data acquisition tools for network analyzers and spectrum analyzers have been developed to facilitate the required data processing. The associated software and hardware have been discussed in section 1.4.2, that refers to various internal reports.
- Poles and zeros are pre-eminently suitable for the analysis and synthesis of complex feedback loops. We started the development of a software tool for simulating root-loci of feedback loops. This program LOCUS has been discussed in various internal reports [113-118] and has provided the tools for developing the basic insight into the feedback theory of chapter 4 and 5.
- Pole-zero extraction is a convenient formalism for cumulative quantification of parasitic effects in measured data. Initially, a variant of the iterative Levenberg-Marquardt algorithm [410,114] has been developed for this purpose. The disadvantage of this algorithm is that starting values are required as input, and that it fails when providing inadequate starting values. Recently we developed linear pole-zero extraction methods as discussed in section 3.1.1. These algorithms require no starting values at all, are much simpler for implementation and have proved to be very robust.

- The pole-zero extraction algorithms facilitate an adequate pole-zero analysis without ignoring parasitic effects. Recently, we developed the missing links of the theory on feedback analysis and synthesis, as described in chapter 4 and 5, and implemented the associated algorithm for taking full advantage of this iterative synthesis.

The progress in performance of our receivers kept pace with the ever increasing performance of our tools for quantifying the cumulative effect of parasitics. An increasing number of parasitic effects have been identified using these tools, resulting in receivers performing in bandwidths as discussed in section 6.2.3.

6.2.3. Bandwidth performance of current-current feedback receivers

The circuit synthesis proposed by Nordholt [406] was used for the initial design of our lightwave receivers. An iterative synthesis improved various sub-circuits one by one. Circuit stripping as well as pole-zero extractions were used for this purpose:

- Some of the quantified parasitic effects are adequately *minimized* by proper redesign of the PCB layout and by adding active decoupling circuits. Some active decoupling circuits had to be removed, since they introduced annoying parasitics.
- The remaining parasitics were cumulated using the pole-zero extraction algorithms as discussed in chapter 4. Dominant parasitics are *neutralized* using adequate compensation networks as discussed in chapter 5.

Various high-performance receivers with third [608,607] and second order [609,610,612,613] feedback loops have been realized, using (parts of) this strategy. All these receivers are constructed using low-cost discrete (SMD) components on low-cost glass-epoxy printed circuit boards in microstrip print layout (see section 1.4.1).

Third order loops. The initial phase of our study was focused on third order feedback loops. The photograph in figure 6.8 on circuit stripping shows one of these prototype receivers. Receivers using third order feedback loops have proved [608] to be feasible for bandwidths exceeding 500 MHz and current gains of more than 100×. These receivers are constructed from discrete components including photo diodes with 1.5~2.0pF photo diode capacitance.

Second order loops. Further increase of bandwidth has not been achieved with third order feedback receivers. The stability compensation was the limiting factor. Various simplified receivers using second order feedback loops have proven feasible for bandwidths of more than 1 GHz and current gains of more than 27×.

The photograph in figure 6.9 shows an implementation of a receiver, using the circuit configuration shown in figure 6.5. Figure 6.10 shows the associated transfer function [609,610,612]. This receiver was configured as a balanced receiver with 1.5 pF total photo-diode capacitance [612], and applied in transmission links for an international ESPRIT 2054 project (UCOL). Similar lightwave receivers have been developed for ATM transmission experiments [108] in an international RACE 2024 project (BAF) or used in various other coherent optical systems [107] (COSNET).

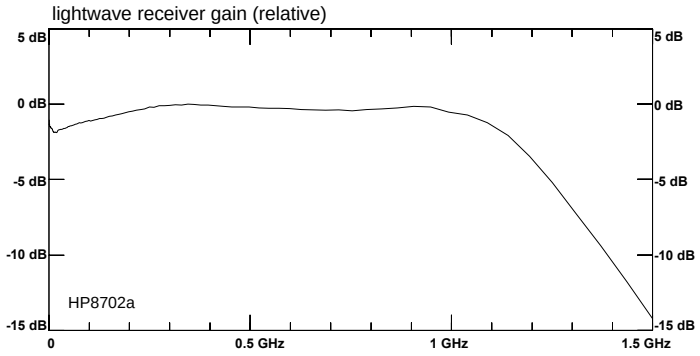


Fig 6.17 *Measured transfer of a lightwave receiver using second order current-current feedback. This receiver, shown in figure 6.5, was configured as a balanced receiver with 1.5 pF total photo-diode capacitance.*

The ultimate bandwidth performance. The results discussed in this section are indicative for how far an iterative synthesis using sophisticated tools can push the overall receiver performance towards physical limits when the technology is restricted to low-cost technology.
In our design example, the actual adjustment of compensation networks was inevitably performed on a trial-and-error base using a circuit simulator. This conventional approach was initially inevitable because our feedback synthesis techniques of section 5.3 were still under development at that time. Therefore it is plausible that the ultimate performance limit has not been reached.
Experimental receivers can be build with bandwidths of more than 2 GHz, although the pass-band ripple of these receivers is too high. Therefore it is plausible that bandwidths of more than 1 GHz are feasible when *all* techniques of chapter 5 are used to support the iterative synthesis of feedback circuits. Further improvements to receiver bandwidth are still undergoing study.

6.3. Iterative synthesis focused on minimal noise

The design of our application example has focused on transfer aspects of the iterative synthesis. It illustrates the value of the transfer-oriented part of our study, as discussed in chapter 4 and 5. This section 6.3 focuses on various noise aspects of iterative synthesis, as introduction to the discussions on noise in chapter 7, 8 and 9.

Wide bandwidth as well as low-noise performance are important aspect of lightwave receivers. One of the major advantages of receivers using current-current feedback is that the associated feedback network is nearly loss-free and therefore almost noise-free. It means that receiver design focused on maximum bandwidth does not seriously deteriorate the overall noise performance. Moreover, the use of *overall* feedback over several amplifier stages improves the overall noise performance. This is because the gain of a first amplifier stage is maximized by avoiding local feedback, and this minimizes the noise contribution of all succeeding amplifier stages.

This section discusses various design aspects of minimizing noise in lightwave receivers by tuning. Again, it emphasizes the importance of circuit stripping techniques and pole-zero techniques when tuning networks are added to the loop, to handle noise tuning as well as feedback stability. The importance of noise characterization as part of an iterative synthesis is discussed in section 6.3.5.

6.3.1. Noise optimization in the absence of tuning

The noise performance of well-designed receivers using overall current-current feedback is in practice determined by the noise of the first amplifying stage. Minimization of equivalent input noise is therefore mainly focused on the first stage.
Figure 6.11 shows an equivalent model of a noisy two-port (first amplifier stage) that amplifies the signal generated by a current source (photo-diode). The two equivalent noise sources are in principle correlated and frequency dependent sources. This two-port noise model is discussed in section 7.3.1. BJT's as well as FET's are suitable for use as the active device in this amplifying two-port.

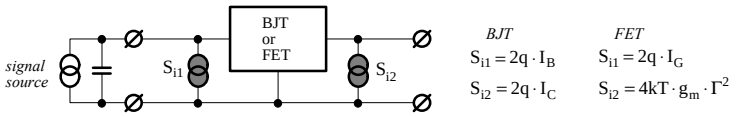


Fig 6.17 *Simplified noise model of the input stage of an amplifier. The two equivalent noise sources are in principle correlated and frequency dependent. The formulas in this figure represent a first order approximation related to the collector bias currents* I_C*, the base bias currents* I_B*, the gate leakage current* I_G *and the transconductance* g_m*. The factor* Γ *is an empirical correction factor:* $\Gamma \approx 1$.

FET's in common source configuration or BJT's in common emitter configuration provide maximal gain and optimal low-noise performance [406]. In these configurations the noise intensity spectra S_{i1} and S_{i2} are nearly white and almost uncorrelated [406]. In a first order approximation S_{i1} equals the shot noise of the base bias-current or gate leakage current, while S_{i2} equals the shot noise of the collector bias-current or the thermal channel noise [406]. In addition, thermal noise of bias resistors must be added to S_{i1} and S_{i2}.
The current gain α of the amplifying two-port reduces the contribution of S_{i2} to the total equivalent input noise. In wideband applications, this current gain $\alpha \approx -(j \cdot f)/(f_T)$ decreases with the frequency as specified by the effective transition frequency f_T of the amplifier stage[4]. Therefore the total equivalent input noise approximates:

$$S_i \approx S_{i1} + S_{i2}/|\alpha|^2 \approx S_{i1} + S_{i2} \cdot |f/f_T|^2$$

Noise measurements, as shown in curve *a* of figure 6.17, demonstrate that the measured noise current ($\sqrt{S_i}$) increases almost linearly with the frequency, as predicted by this

[4] Note that the effective transition frequency of the *input stage* is less than the transition frequency of the individual active devices. Its value is lowered by the photo diode capacitance and all other parasitic capacitances at the input. This holds especially when FET's are used because the transconductance of FET's is usually significantly lower than the transconductance of BJT's with equal transition frequency.

formula. This approximation often holds for FET's as well as for BJT's in wideband lightwave receivers. At relatively low frequencies the current gain a of FET's is extremely high, which makes them in these cases superior in noise performance to BJT's. At relatively high frequencies this preference is not so obvious since in these situations the influence of ω_T is dominant.

Noise optimization is primarily a matter of finding an optimal combination of f_T, S_{i1} and S_{i2} by selecting an optimal active device and optimal bias conditions [606]. Nordholt [406] has discussed this general procedure in detail from which we concluded that FET's are preferable to BJT's in our design example because of their low S_{i1}.
The transition frequency f_T is an important parameter for low-noise design, and parasitic capacitances such as photo diode capacitance easily deteriorate this transition frequency. This holds especially when FET's are used in combination with diode capacitances as high as 1.5 pF. Specifically in this case, the circuit stripping techniques of section 6.2.1 and the circuit model extraction algorithms of section 3.1 and 3.2 are of primary importance for optimizing the noise performance of the amplifiers.

6.3.2. Noise tuning in absence of overall feedback

A more complex manner of improving the overall noise performance may be found in increasing the current gain α of the first amplifier stage using resonance techniques [601,603,604]. Figure 6.12 illustrates various tuning networks for connecting signal current sources (photo diode) to the input stage of receiver front-ends. We may distinguish the following tuning examples:

- *Shunt tuning*, as shown in figure 6.12a, uses a band-pass transfer function and cancels the capacitive diode- and input impedance within a small frequency band. Below this band the signal is shorted to ground making this type of tuning unsuitable for wideband applications extending relatively low frequencies.
- *Series tuning*, as shown in figure 6.12b, uses a low-pass transfer function, peaking in the vicinity of a corner frequency. When this frequency is equal to the bandwidth of interest, series tuning improves the noise performance in the high end of the pass band and deteriorates it above this band. Noise measurements, as shown in curve *a* in figure 6.17, illustrate how effective this approach can be.
- *Higher order tuning networks*, as shown in figure 6.12c, may, by introducing additional degrees of freedom, extend the tuning bandwidth when properly adjusted. The illustration depicts a ladder configuration, although various other combinations of inductors and capacitors are applicable.
- *Transformer tuning*, as shown in figure 6.12d, is just another version of higher order tuning.

These examples are all restricted to lumped elements. In practice the values of the tuning inductors are very low (e.g. below 50 nH for 1 GHz applications). Distributed tuning networks, such as short transmission lines, stubs and dielectric tuning tabs (e.g. ε_r>100), are therefore viable alternatives.

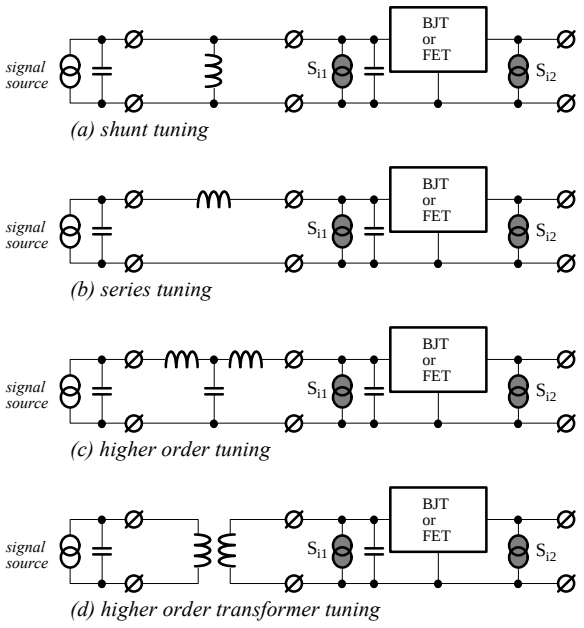


Fig 6.17 *Various examples of tuning networks for improving the overall noise performance.*

At the course of this study, experiments have been carried out with a variety of front-end receiver and tuning configurations. For an overview of various tuning configurations, see Jacobsen and Kan [603,604] or van der Vleut [611]. Figure 6.13 and 6.14 show a series tuned front-end, without feedback, using a transmission line and an additional dielectric tuning tab [611]. Figure 6.15 shows a front-end without feedback using higher order tuning networks.

Parasitic effects play a dominant role in tuned front-ends, and a tuning network consists in part of parasitic elements. Moreover, most elements of a tuning network cannot be adjusted when the actual value differ from the desired value. This emphasizes the importance of precise control of these parasitic elements to make them reproducible and accurately known.
The parasitic effects of the tuning networks have been quantified by various techniques as described in chapter 2, so that iterative synthesis may be effectively applied.

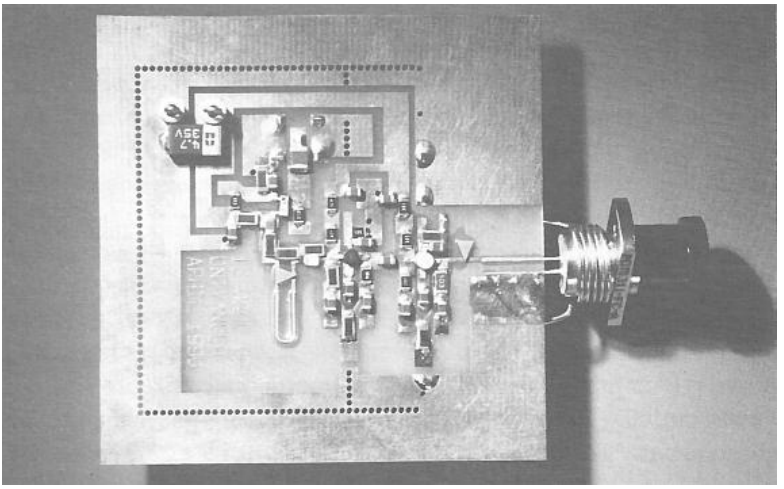


Fig 6.13 *Tuned front-end (without feedback) using a transmission line and a dielectric tab as tuning element.*

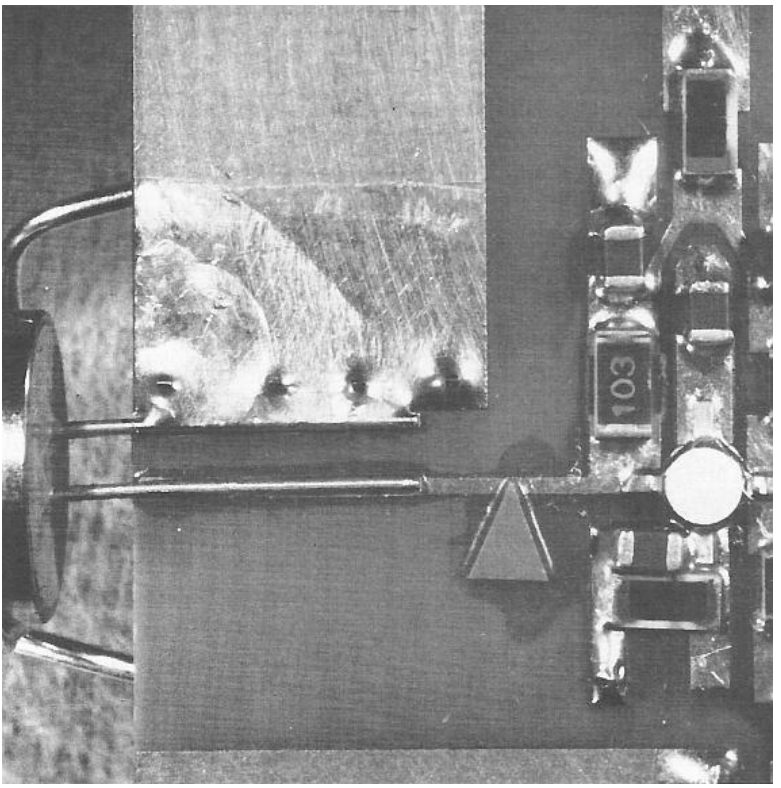


Fig 6.14 *Close-up of the tuned receiver shown in figure 6.13.*

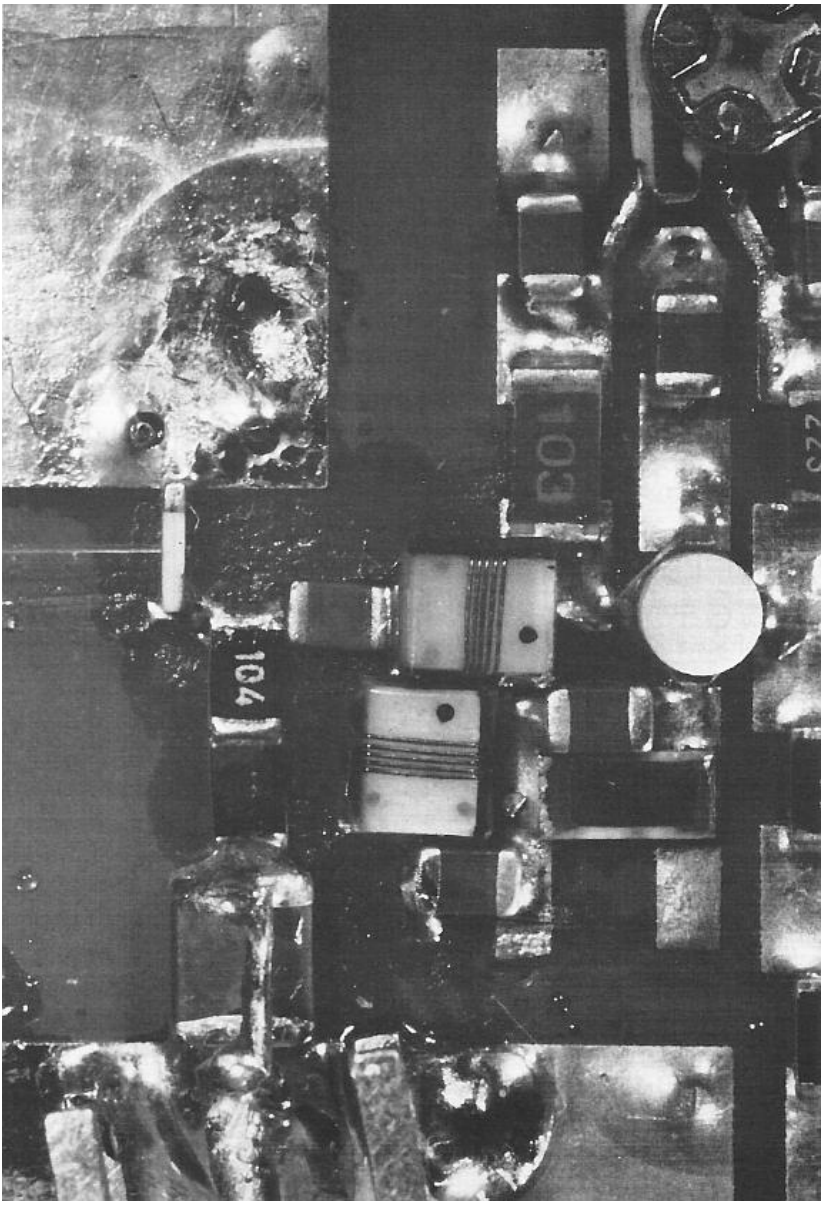


Fig 6.15 *Close-up of a tuned front-end (without feedback) using two wound inductors and a parasitic third inductor as tuning element.*

6.3.3. Noise tuning in combination with overall feedback

Tuning networks improve noise performance by modifying the current gain of the first amplifier stage. The principle drawback of noise tuning is that it deteriorates the transfer function of the lightwave receiver. External equalizers are required to eliminate this effect.

Overall feedback loops can make the use of equalizers superfluous. On the other hand, tuning networks affect the loop-gain and may endanger the overall stability of the feedback loop. In practice, overall feedback loops in combination with input tuning are commonly avoided.

This study has demonstrated [613] the viability of using higher order feedback in *combination* with input tuning. Tuned receivers have been realized using second order current-current feedback loops with bandwidths up to 900 MHz. Their noise performance is discussed in section 6.3.4.

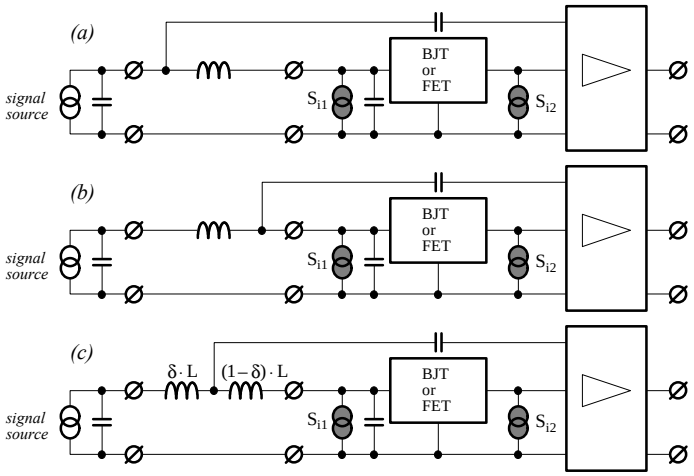


Fig 6.17 *Typical examples incorporating input tuning in the feedback loop to improve the overall noise performance in lightwave receivers. When example* c *is well-designed the feedback current is frequency independently distributed over the source impedance and the input impedance.*

In wideband design, the manner of interconnecting the feedback networks to the tuned input is the determinative factor in establishing feasibility. Figure 6.16 shows three typical examples. Configuration *c* is to be preferred [613] in wideband feedback applications for the following reasons:

- Figure 6.16a shows a configuration in which the serial tuning inductor is placed within the feedback loop. In case of infinite loop-gain, the overall transfer (output signal / photo current) is fully controlled by feedback and the tuning inductor will not deteriorate the overall transfer function. This is an important advantage.
  In practice, however, the tuning inductance plays a significant role at frequencies close to the high end of the receiver pass band. The loop-gain is then relatively low, and the tuning network inevitably degrades the overall transfer. Furthermore, in

most wideband applications the loop stability cannot be compensated. This is a serious disadvantage.

- In figure 6.16b the serial tuning inductor is placed outside the feedback loop. In the case of ideal photo-diodes with infinite output impedance, the loop-gain is not affected and the serial tuning inductor does not endanger the stability of the feedback loop.
  In practice, the photo-diode shunt capacitance in combination with the tuning inductor lowers the loop-gain. The loop stability cannot then be compensated in most wideband applications. In this situation, the transfer function as well as the loop-gain are deteriorated by the tuning network.
- Figure 6.16c depicts a superior solution that eliminates the loop-gain deterioration. When properly adjusted, the feedback current is frequency <u>in</u>dependently distributed over photo-diode capacitance c_d and input capacitance c_g of the input stage. In the case that $c_d=c_g$, the tuning inductors $\delta\cdot L$ and $(1-\delta)\cdot L$ are equal. This alternative solution enables stable operation of higher order feedback loops in combination with input tuning.

This discussion is indicative of the complexity involved in using higher order feedback loops in combination with noise tuning in wideband applications. Parasitic effects play a dominant role. *Iterative* synthesis is required to facilitate stable feedback operation as well as adequate noise tuning.
In the design of the lightwave receivers described in this text, circuit parameters for adequate circuit simulation are extracted from circuit stripping techniques. The use of root-locus and pole-zero tools, as implemented in our SABEL-CAE [111] design environment, facilitated the design of wideband higher-order feedback loops.

6.3.4. Noise performance of current-current feedback receivers

The measurements in figure 6.17 show the equivalent input noise achieved for our lightwave receiver design examples. It represents the noise of lightwave receivers [613] using second order current-current feedback, a balanced pair of photo-diodes (1.5 pF) and an FET as input stage.
Curve *a* depicts the equivalent noise current ($=\sqrt{S_i}$) of a receiver front-end without input tuning. This measured curve is superimposed on a curve: $S_i=S_{i1}+(f/f_T)^2\cdot S_{i2}$, as explained in section 6.3.1. The quantities S_{i1}, S_{i2} and f_T are parameters of the associated noise and transfer model. Curve *b* represents the noise current of a similar receiver using series tuning.
The average noise of the tuned front-end equals 3 pA/√Hz. This noise level is as low as the thermal noise current of a 1.8 kΩ resistor or as the shot noise associated with a dc-current of 28 μA. These results have been achieved with low-cost components photo-diode capacitance in excess of 1.5pF. Comparable state-of-the-art receivers have been described using superior higher-cost components such as photo-diodes with lower shunt capacitance and avalanche photo diodes (APD's). This bodes well for the use of sophisticated design strategies to push overall receiver performance towards physical limits.

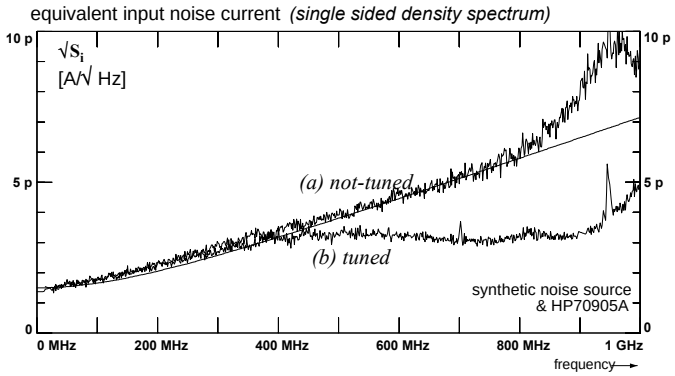


Fig 6.17 *Measured input noise of two lightwave receivers [613], using the measurement techniques discussed in section [8.4] It represents the noise observed from an electrical reference plane, between photo-diode and amplifier.*

Reliability of noise simulations

The prediction of noise in receivers without tuning is reasonably succesful when simple noise models are used in combination with transfer parameters extracted from measurements. For instance, the minimum noise level ($\sqrt{S_{i1}}$=1.5 pA/√Hz) is restricted by the thermal noise of the gate bias resistor[5] in the feedback network and by the gate leakage current of the input FET. Noise increases with frequency, may be predicted by taking into account the total input capacitance (photo-diode and FET) and the FET transconductance[6]. The noise peak at the high end of the pass band probably originates from a parasitic tuning effect, that is to be identified.

Reliable prediction of the noise in receivers with tuning requires more sophisticated models. The tuning dip in figure 6.17 is not as deep as expected based on noise calculations using simple models. One of the reasons is that thermal noise effects in lossy tuning inductors have not been taken into account. Another reason is that *estimated* FET models were used, which probably requires further refinement.

6.3.5. The role of noise measurements in an iterative synthesis

Most of section 6.3 is focused on low-noise design using *measured* transfer parameters (circuit stripping) in combination with *estimated* noise parameters (the formulas in figure 6.11). This is because adequate instruments for transfer measurements on microwave and lightwave receivers are commercially available. Currently (1994), this does not hold for optical noise measurements on lightwave receivers, and is only partly true for electrical noise measurements[7].

---

[5] The thermal noise of a 10kΩ resistor is 1.3 pA/√Hz.

[6] The parameters, reconstructed from noise and transfer measurements are: S_{i1}=1.5pA/√Hz, S_{i2}=34pA/√Hz, f_T=5.2GHz, C_{tot}=2.5pF (diode=1.5pF, FET=0.8pF, stray=0.2pF) , g_m=82mA/V.

[7] We note that instruments for full two-port noise measurements are commercially available. They focus, however, on microwave applications.

It is obvious that designing receivers based on estimated noise parameters yield sub-optimal results. Therefore, an iterative synthesis must also be based on *measured* noise parameters. The basic aspects are discussed below.

Noise measurements. Measurement of overall receiver noise is required to validate the noise performance predicted by estimated noise models. In simple situations, such as receivers without tuning, this approach has proven adequate. It provides some understanding of parasitic noise effects required for optimal low-noise design.
When tuning networks are involved, our measurements of overall receiver noise indicate a deviation between predicted and measured noise. Two-port noise measurements on individual devices, such as the input FET, are required to quantify parasitic noise effects that are inadequately modeled or that not have been taken into account. This would supplement our understanding of parasitic noise effects and enable further improvement of front-end design. Up to 5 dB additional improvement in wideband noise level is expected [613] for our design examples when the theoretical optimum has been achieved with similar components

Noise simulations. Simple[8] noise simulations have proven adequate when designing optimal low-noise receivers in the absence of noise tuning. Thermal noise effects due to lossy tuning inductors were not taken into account in our simulation of tuned receivers. Further, the noise in the input FET was assumed to be white and uncorrelated.
When the simulation is based on reliable noise models for FET's and BJT's, extracted from two-port noise measurements, then these sources are probably correlated. Therefore more sophisticated noise simulations are required for further improvement of tuned receiver noise.

New developments. The second part of this study (chapter 7-9) is focused on algorithms for improved noise simulation, algorithms for noise parameter extraction of measured data, and on techniques for noise measurements
Chapter 7 discuses a general theory on noise, to facilitate sophisticated noise simulations of arbitrary linear circuits. It illustrates the extraction of thermal noise effects from transfer measurements.
Chapter 8 introduces various novel noise measurement techniques. It illustrates the measurement of electrical noise of *optical* receiver and full two-port noise characterization of semiconductor devices.
Chapter 9 describes the development of a novel measurement instrument to facilitate the desired noise measurements. This lightwave instrument generates white noise over tens of GHz.

[8] Simple noise calculations use AC transfer analysis for a finite number of uncorrelated white noise sources. Circuit simulators supporting this method calculate the RMS sum of all white noise sources at a specified output node. This value is then divided by the gain to calculate the equivalent input noise. Pspice® [128] is an example of a circuit simulator using this approach. Modern microwave simulators use a more complete noise algorithm.

6.4. Conclusions

The application of the tools of this study in the support of iterative circuit synthesis for lightwave receiver design has been discussed. First cut receiver design was improved by extracting various circuit parameters from measured data. The extracted values provide a deeper understanding of parasitic effects and enable a designer using iterative synthesis to obtain optimal circuit performance.

Receiver performance

An adequate classification method was used to select an optimal lightwave receiver configuration based on current-current feedback. The examples make use of higher order feedback loops, demonstrating the applicability of higher order feedback in broad band design. Using iterative synthesis techniques, we developed the first lightwave receiver with third order current-current feedback over more than 500 MHz bandwidth [608]. The feasibility of second order feedback loops in combination with noise-tuning networks has been demonstrated over more than 1 GHz in bandwidth. An average noise level of 3 pA/√Hz has been achieved over this frequency band in combination with photo diodes having 1.5 pF shunt capacitance.

This performance is indicative of the ability of iterative synthesis using state-of-the-art tools to push overall receiver performance towards physical limits, even when low-cost technology is mandated. It is reasonable to expect that when all the tools of this study are applied, greater bandwidths will prove feasible.

All of the design examples of this chapter have been realized using discrete components mounted on low-cost glass-epoxy prints (see section 1.4.1). Although neither integrated circuit solutions thin film solutions have been investigated as yet, the application of the methods described in this book should prove applicable. Similar conclusions hold for other technologies, such as chips, although on a different (frequency) scale.

iterative synthesis focused on maximal bandwidth

Section 6.2 was focused on feedback transfer aspects of the design example. This study resulted in the development of *circuit stripping* techniques to quantify parasitic effects in the feedback loop. Circuit stripping is a structured method for locating inadequately modeled circuit elements. It enables the extraction of realistic model parameters from measurements, as described in chapter 2.

Parasitic effects that are significant in sub-circuits and devices are not necessarily significant in the overall feedback loop. This study resulted in various *pole-zero techniques* to cumulate the effect of various parasitics in the overall feedback loop. It enables the extraction of dominant poles and zeros in the loop, as described in chapter 3.

The dominant poles and zeros have been compensated by adequate compensation networks, as described in chapter 5. Design of the compensation network was initially performed on a trial-and-error base using a circuit simulator. New *compensation algorithms*, introduced in chapter 5, facilitate the structured design of the compensation networks as well as the devising of new compensation concepts.

iterative synthesis focused on minimal noise

Section 6.3 focused on noise aspects of the design example. Detailed knowledge of various parasitic effects enables the designer of lightwave receivers to combine noise tuning networks with higher order feedback loops.

Simple noise simulations on tuned receivers have been shown to be only moderately reliable. This was because thermal noise effects in the tuning elements and noise correlation in the active devices are not taken into account. The *general noise theory* in chapter 7 facilitates a more reliable simulation and in principle enables the design of improved tuning networks.
Noise models with estimated parameters were used in the noise simulation. The novel measurement techniques of chapter 8 to measure the overall *receiver noise* facilitate the identification of relevant parasitic noise effects. Noise models may be refined and tuning elements adjusted to improve the low-noise performance of the receiver. Ultimate performance requires full *two-port noise measurements* on the individual devices to insure reliable noise simulations. Associated measurement techniques are discussed in chapter 8, using a synthetic noise generator as described in chapter 9.